

Uncertainty assessment of potential evapotranspiration in arid areas, as estimated by the Penman-Monteith method

HUA Ding^{1,2}, HAO Xingming^{1,2*}, ZHANG Ying^{1,2}, QIN Jingxiu^{1,2}

¹ State Key Laboratory of Desert and Oasis Ecology, Xinjiang Institute of Ecology and Geography, Chinese Academy of Sciences, Urumqi 830011, China;

² University of Chinese Academy of Sciences; Beijing 100049, China

Abstract: The Penman-Monteith (PM) method is the most widely used technique to estimate potential worldwide evapotranspiration. However, current research shows that there may be significant errors in the application of this method in arid areas, although questions remain as to the degree of this estimation error and how different surface conditions may affect the estimation error. To address these issues, we evaluated the uncertainty of the PM method under different underlying conditions in an arid area of Northwest China by analyzing data from 84 meteorological stations and various Moderate Resolution Imaging Spectroradiometer (MODIS) products, including land surface temperature and surface albedo. First, we found that when the PM method used air temperature to calculate the slope of the saturation vapor pressure curve, it significantly overestimated the potential evapotranspiration; the mean annual and July–August overestimation was 83.9 and 36.7 mm, respectively. Second, the PM method usually set the surface albedo to a fixed value, which led to the potential evapotranspiration being underestimated; the mean annual underestimation was 27.5 mm, while the overestimation for July to August was 5.3 mm. Third, the PM method significantly overestimated the potential evapotranspiration in the arid area. This difference in estimation was closely related to the underlying surface conditions. For the entire arid zone, the PM method overestimated the potential evapotranspiration by 33.7 mm per year, with an overestimation of 29.0 mm from July to August. The most significant overestimation was evident in the mountainous and plain non-vegetation areas, in which the annual mean overestimation reached 5% and 10%, respectively; during July, there was an estimation of 10% and 20%, respectively. Although the annual evapotranspiration of the plains with better vegetation coverage was slightly underestimated, overestimation still occurred in July and August, with a mean overestimation of approximately 5%. In order to estimate potential evapotranspiration in the arid zone, it is important that we identify a reasonable parameter with which to calibrate the PM formula, such as the slope of the saturation vapor pressure curve, and the surface albedo. We recommend that some parameters must be corrected when using PM in order to estimate potential evapotranspiration in arid regions.

Keywords: Penman-Monteith; parameter correction; surface temperature; albedo; Northwest China

Citation: HUA Ding, HAO Xingming, ZHANG Ying, QIN Jingxiu. 2020. Uncertainty assessment of potential evapotranspiration in arid areas, as estimated by the Penman-Monteith method. *Journal of Arid Land*, 12(1): 166–180. <https://doi.org/10.1007/s40333-020-0093-7>

1 Introduction

*Corresponding author: HAO Xingming (E-mail: haoxm@ms.xjb.ac.cn)

Received 2019-05-13; revised 2019-12-02; accepted 2019-12-25

© Xinjiang Institute of Ecology and Geography, Chinese Academy of Sciences, Science Press and Springer-Verlag GmbH Germany, part of Springer Nature 2020

The evapotranspiration process includes water surface evaporation, soil evaporation, vegetation transpiration and intercepted precipitation within the canopy vegetation. This process is an important aspect of surface water-heat balance and an important indicator of vegetative growth and crop yield (Zhang et al., 2012). Two terms are commonly used in hydrology: actual evapotranspiration and potential evapotranspiration. The former represents the true evaporation from the surface to the atmosphere, while the latter represents the demand for atmospheric evaporation (Anabalón and Sharma, 2017). The instrument used to measure actual evapotranspiration is costly and difficult to maintain (Zhao et al., 2013); consequently, valid evapotranspiration data are difficult to obtain directly. Therefore, potential evapotranspiration has become a key parameter to reflect regional evaporation capacity. Over recent years, global temperatures have continued to rise; as a result evaporation has increased and water cycles have been affected (Peng et al., 2013). Potential evapotranspiration, as an important component of water balance, plays an important role in the management of water demand in crops (Koffi et al., 2018), the monitoring of drought and flood (Tirivarombo et al., 2018), and improvements in the efficiency of water use (Wei et al., 2018). The demands made by these important applications, are associated with higher requirements when estimating the accuracy of potential evapotranspiration.

The first measurement of evapotranspiration in a basin was reported by Harley (1964); this measurement was taken in an evaporating dish. The theoretical framework for the estimation of potential evapotranspiration can be traced back to the 'Dalton evaporation theory' in 1802, which provided a clear physical meaning to the theory of watershed evaporation (Ci et al., 2005). Following the development of estimation methods and technology, the current methods for estimating potential evapotranspiration can be classified into five basic methods: comprehensive, temperature, radiation, water balance and mass conduction (Xu and Singh, 2001). At present, the most widely used method is the comprehensive method, as represented by the Penman-Monteith (PM) method. The PM method can be used in many regions of the world without excessive parameterization (Zhang et al., 2016; Tegos et al., 2017) and is recommended by the Food and Agriculture Organization of the United Nations (FAO) as the standard method for calculating potential evapotranspiration (Li et al., 2007). This method defines the evapotranspiration rate of the reference canopy as potential evapotranspiration, and sets the reference crop height, surface resistance and reflectance, to a fixed value that is similar to grassland that is completely covered by vegetation (Ogles and Gutowski, 2005). Although the PM method is still widely used for the estimation of reference crop evapotranspiration (ET_0) (Ficklin et al., 2014) under extremely unstable boundary layer conditions, the actual evapotranspiration value will become smaller than the value estimated by the original PM formula. At the same net input energy, the sensible heat flux in arid regions is much larger than the sensible heat flux under neutral conditions (Ogles and Gutowski, 2005), and the PM method overestimates the aerodynamic component of ET_0 , leading to obvious flaws in energy balance closure in northern China (Hao et al., 2018). Therefore, large errors may arise when potential evapotranspiration is calculated by the PM method in arid regions. In a previous study, Westerhoff (2015) estimated the uncertainty of ET_0 and showed that temperature is a sensitive factor and an important source component for PM error. There are still problems in the albedo parameterization of different underlying surfaces in arid areas (Chen et al., 2014). Recent research has shown that there are two possible sources of estimation error for the PM method. Firstly, there is a large difference between surface temperature and air temperature in sparse areas of vegetation (Wan and Li, 2008), thus resulting in a significant difference between the slope of the saturation vapor curve of the PM formula in areas with sparse vegetation and areas with good coverage of vegetation (Dhungel et al., 2014). Secondly, a large difference exists in surface albedo in areas with different vegetation coverage (Chen et al., 2014), even if the surface albedo in the same area is completely different during the year (Fugazza et al., 2016). Consequently, it is very challenging to estimate ET_0 in arid zones in an accurate manner. Fortunately, remote-sensing technology can now obtain ground parameter data in an accurate manner and on a regional-scale (Mallick et al., 2014). This creates a new opportunity for the PM method to accurately estimate the potential evapotranspiration under an unstable underlying surface.

In a previous paper, Chen et al. (2018) evaluated the uncertainty of the evapotranspiration

estimation in the temperate meadow region of Inner Mongolia, by comparing the PM formula with the eddy covariance method. The data arising from this study showed that the PM formula overestimated evapotranspiration by 12.1% and 12.8% on the half-hour and daily scales, respectively. In another study, Raoufi and Beighley (2017) calculated potential evapotranspiration using the PM method and remote sensing data, including such as leaf area index, land surface temperature and albedo. Results were then compared to *in-situ* measurements; the root mean square errors, on the daily and monthly scales, were 0.81 and 0.77 mm/d, respectively. Although the mean global difference between MOD16 (MODIS Global Evapotranspiration Project) and ET (evapotranspiration) estimates was only 0.2 mm/d, local temperature-derived vapor pressures most likely contributed to these differences, particularly in energy- and water-limited regions. However, what proportion of this uncertainty is caused by the PM method in the arid zone (taking arid regions of Northwest China as an example), however, remains unknown.

Therefore, in this study, we used the arid areas of Northwest China as an example to correct the two parameters, the saturation vapor pressure and albedo, utilized by the PM method. Next, we calculated the influence of each parameter on the resultant data and compared the adaptability of this method to different surface conditions. Finally, we determined the error associated with the PM method in arid regions of Northwest China by correcting these two parameters. This study further improved the calculation accuracy of potential evapotranspiration within the study area. We recommend that these two parameters must be corrected in arid areas in order to reduce errors.

2 Study area and data collection

2.1 Overview of the study area

The arid areas of Northwest China (35°–50°N, 73°–106°E; Fig. 1) are located deep in the hinterland, covering an area of approximately 2.5×10^6 km², thus accounting for approximately one quarter of China's land area. This arid region has a typical continental arid climate with strong evaporation, and the annual mean potential evaporation exceeds 1000 mm (Li et al., 2013). The topography and geomorphology of this area are complex and varied, featuring mountains, plateaus, deserts and basins. There are not many plants in this region; rather the area is dominated by trees, shrubs and semi-shrubs that are degraded by dry leaves. The mean annual precipitation in this area is less than 400 mm and is mostly concentrated in mountainous areas; the precipitation in the plain area is less than 160 mm. The arid region of Northwest China is known to be one of the most sensitive areas to global changes (Chen et al., 2015, 2016).

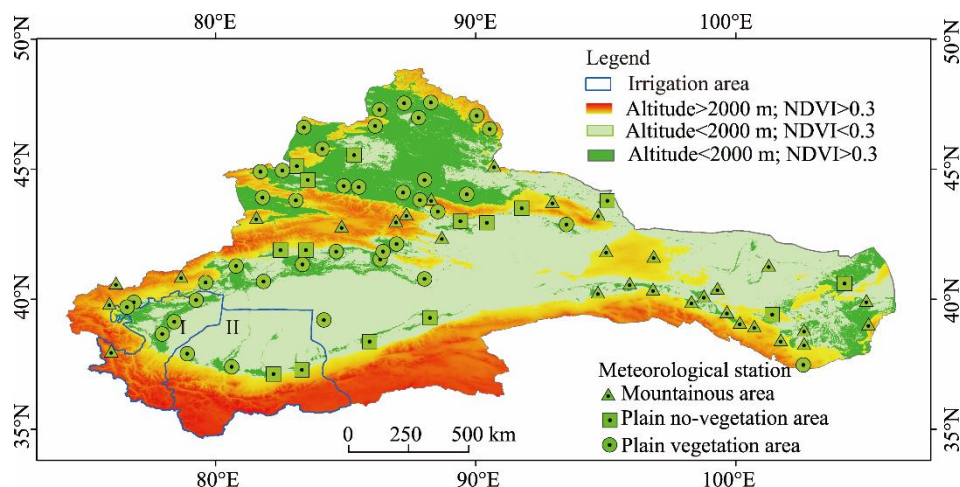


Fig. 1 Study area and the distribution of meteorological stations. I, Kizilsu Kirgiz irrigation area; II, Hotan irrigation area; NDVI, Normalized Difference Vegetation Index.

Although the area of oasis accounts for a small proportion of the entire arid area of Northwest

China, these areas carry 90% of the population, and supply 95% of the total economic output (Li et al., 2011). These areas also feature the most concentrated agricultural production (Zhang, 2003). In order to explore the impact of estimation error when calculating potential evapotranspiration to determine crop water demand, we selected two agricultural irrigation areas in Hotan Prefecture and Kashgar Prefecture; the main crops in these areas are wheat, corn and cotton.

2.2 Data collection

The meteorological data used in this study came from 84 national meteorological station observatories in arid regions of Northwest China. The study period was defined as 2003 to 2017. The observation factors included daily mean temperature, daily maximum temperature, daily minimum temperature, mean air pressure, relative humidity, wind speed, and sunshine hours. We downloaded these data from the China Meteorological Data Service Centre website (http://data.cma.cn/data/cdcdetail/dataCode/SURF_CLI_CHN_MUL_DAY_V3.0.html). The terrain of the study area is complex and diverse. Therefore, according to the altitude and Normalized Difference Vegetation Index (NDVI) corresponding to the meteorological station, we divided each meteorological station class into three types: a plain non-vegetation area (altitude <2000 m, NDVI<0.3), a plain vegetation area (altitude<2000 m, NDVI>0.3), and a mountainous area (altitude>2000 m, NDVI>0.3); the specific classification is shown in Figure 1.

The remote-sensing products selected for this study were derived from MODIS (Moderate Resolution Imaging Spectroradiometer) sensors, including LST (land surface temperature), albedo and NDVI. The specific parameters for these data are shown in Table 1. We downloaded all remote-sensing data from the official website NASA (National Aeronautics and Space Administration of the USA).

Table 1 Resolutions of major Moderate Resolution Imaging Spectroradiometer products

Parameter	Type	Time resolution (d)	Spatial resolution	Source
LST	MYD11A1	1	1000 m×1000 m	NASA
Albedo	MCD43A3	1	500 m×500 m	NASA
NDVI	MYD13A1	16	500 m×500 m	NASA

Note: LST, land surface temperature; NDVI, Normalized Difference Vegetation Index; NASA, National Aeronautics and Space Administration of the USA.

3 Methods

The Penman-Monteith (PM) model assumes that the underlying surface conditions of the estimation zone are stable, the reference crop height is 0.12 m, and the fixed surface air impedance is 70 s/m; these assumptions satisfy the energy balance of radiation and sensible heat, and the aerodynamic transfer equation. The specific calculation formula is shown in Equation 1 (Allen et al., 1998),

$$ET_0 = \frac{0.408\Delta(R_n - G) + \gamma \frac{900}{T + 273} \mu_2 (e_s - e_a)}{\Delta + \gamma(1 + 0.34\mu_2)}, \quad (1)$$

where ET_0 represents the reference crop evapotranspiration rate (mm/d); R_n represents the surface net radiation amount (MJ/(m²·d)); G represents the soil heat flux (MJ/(m²·d)); Δ represents the slope of saturation vapor pressure curve (kPa/°C); μ_2 represents the wind speed at 2 m high (m/s); γ represents the psychrometric constant (kPa/°C); e_s represents the saturation vapor pressure (kPa); and e_a represents actual vapor pressure (kPa).

In this study, we corrected the slope of the saturation vapor pressure curve and surface albedo of the PM formula, based on the principle of the PM method to evaluate the uncertainty of estimating the evapotranspiration in arid areas.

3.1 Correcting the slope of the saturation vapor pressure curve

The land surface temperature has proven difficult to obtain in the past, so the parameterized equation (Eq. 2), based on air temperature, is widely promoted. In the PM formula, the Δ calculation is

simplified to the assumption that the surface is a stable neutral atmosphere as below:

$$\Delta = \frac{4098[0.6108 \exp(\frac{17.27+T_a}{T_a+273.3})]}{(T_a+273.3)^2}, \quad (2)$$

where T_a represents the air temperature ($^{\circ}\text{C}$).

However, the Δ varies greatly in areas where vegetation is sparse, and in areas that are well covered; this is because the land surface temperature differs significantly from the air temperature in areas with poor vegetation coverage (Wan and Li, 2008; Shen and Leptoukh, 2011). The development of remote sensing technology can accurately obtain the surface temperature value, which provides an effective way to rehabilitate the Δ parameter.

In the original complete PM formula, according to the physical meaning of the slope of saturation vapor pressure, Δ should be obtained by the saturation vapor pressure between the air temperature and the land surface temperature (Penman, 1948; Allen et al., 2006; Dhungel et al., 2014) as shown in Equations 3 and 4.

$$\Delta(f = T_s, T_a) = \frac{e_{\text{sur}}^0 - e_{\text{air}}^0}{T_s - T_a}, \quad (3)$$

$$e_x^0 = 0.6108 \times \exp(\frac{17.27(T_x - 273)}{T_x - 35.86}), \quad (4)$$

where T_s represents land surface temperature ($^{\circ}\text{C}$); e_{sur}^0 represents saturation vapor pressure (kPa) calculated using land surface temperature; e_{air}^0 represents saturation vapor pressure (kPa) calculated using air temperature; and e_x^0 represents the saturation vapor pressure (kPa) at the temperature x ($^{\circ}\text{C}$).

3.2 Albedo correction

Because the PM method assumes the ideal underlying surface condition, we set the surface albedo to 0.23. In arid and semi-arid regions, however, vegetation is sparse and changes are obvious throughout the year; consequently this is far from achieving the ideal grassland state, but without experiencing water shortage. Therefore, to improve the accuracy of this model, our study restored the actual surface albedo with reliable remote-sensing data using the MODIS surface albedo product, MCD43A3 (Eq. 5).

$$\alpha = \frac{\text{BSA}}{1000}, \quad (5)$$

where α represents albedo, while BSA is the albedo estimated from black-sky, direct beam.

3.3 Calculation of crop water demand

This study used the crop coefficient method, as recommended by the FAO, to calculate the crop water requirement (Shen et al., 2013) as shown in Equation 6.

$$\text{ET}_c = K_c \times \text{ET}_0 \quad (6)$$

where ET_c represents crop water demand, while K_c represents the crop coefficient. The crop coefficients of the major crops, in different growth stages of the two oases, were those recommended by the FAO (Table 2).

4 Results

4.1 Uncertainty caused by the slope of the saturation vapor pressure curve

Compared with the $\text{ET}_0 - \Delta$ (potential evapotranspiration corrected by the slope of saturation vapor pressure curve), the $\text{ET}_0 - \text{PM}$ (potential evapotranspiration that was estimated by the original PM formula) significantly overestimated the local potential evapotranspiration (Fig. 2). On the annual

Table 2 Crop coefficients of the major crops in different growth stages

Crop	Growth stage						
	April	May	June	July	August	September	October
Rice	0.000	0.856	1.540	1.470	0.280	0.000	0.000
Wheat	0.590	1.280	1.028	0.210	0.000	0.000	0.000
Corn	0.267	1.190	1.559	0.790	0.000	0.000	0.000
Cotton	0.351	1.010	1.255	1.250	1.000	0.735	0.300
Walnut	0.722	1.216	1.343	1.065	0.829	1.288	0.273
Fruit forest	0.549	1.158	1.352	1.263	1.190	0.850	0.113

scale, more than 70% of the sites in the study area were associated with an overestimated ET_0 (Fig. 2a). The mean annual ET_0 was overestimated by 7.4% (83.9 mm), and the sites that were overestimated, and most significant, were overestimated by more than 35% each year. The overestimation of ET_0 during the year was mainly concentrated in the months of July and August. During this period, more than 80% of the sites in the study area had an ET_0 -PM greater than the ET_0 - Δ (Fig. 2b); this level of overestimation was significant, with an average of 12.2% (36.65 mm).

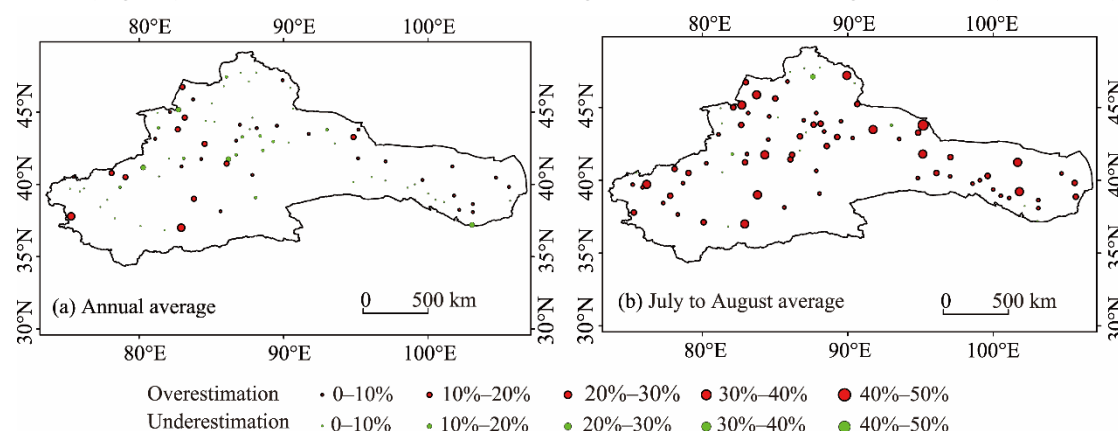


Fig. 2 Overestimation and underestimation of ET_0 -PM (potential evapotranspiration that was estimated by the original Penman-Monteith (PM) formula ($\Delta(f=T_a)$) and ET_0 - Δ (potential evapotranspiration corrected by the slope of the saturation vapor pressure curve) ($\Delta(f=T_a, T_s)$) in 84 meteorological stations during 2003–2017

The slope of the saturation vapor pressure curve causes the PM formula to significantly overestimate in different regions. The primary manifestation of this was that the plain non-vegetation areas had a greater degree of overestimation than the mountainous areas and the plain vegetation areas (Fig. 3). Across the entire study area, the greatest difference was between the surface temperature and the air temperature in the plain non-vegetation area. The error between the Δ based on air temperature fitting and the value after correction was also the largest. These factors are responsible for large errors produced by the PM in such areas, with an overestimation of 180.6 mm/a, accounting for 16.3% of the annual evaporation. This overestimation was more pronounced in July and August, with a mean overestimation of 59.2 mm/a, and an overestimation of 17.3% (Fig. 3g). The second largest degree of overestimation was in the mountainous areas; despite the fact that some sites were underestimated, the overall scenario was still overestimated. The mean annual overestimation was 80.30 mm, representing an overestimation of 6.8%. Similarly, the overestimation in July and August was even higher; the number of overestimated sites also increased. The mean overestimation was 33.5 mm/a, which accounted for 11.3% of the total potential evaporation in these two months (Fig. 3i). The vegetation coverage of the site in the plain vegetation area was closest to the PM preset condition. Although the surface temperature was similar to the air temperature, the Δ error could not be ignored. The PM model overestimated potential evapotranspiration by 69.3 and 26.5 mm/a in July and August, respectively. The margin of difference was 4.7% for the year, and 9.1% for July and August (Fig. 3h).

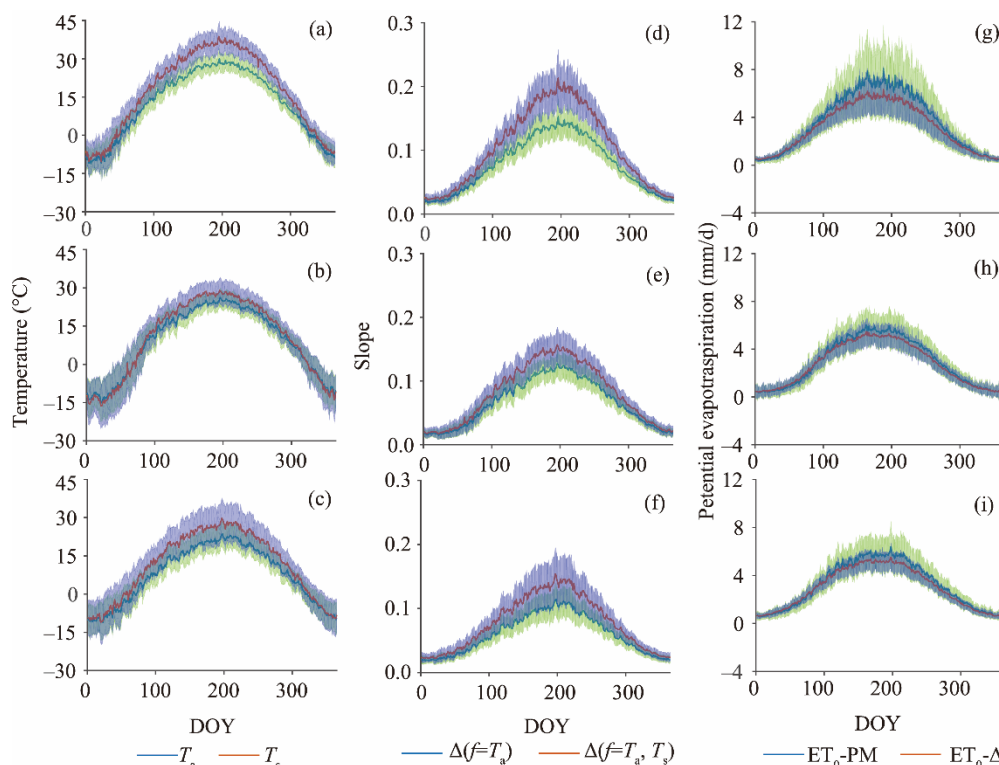


Fig. 3 Annual variations between T_a (air temperature) and T_s (land surface temperature), $\Delta(f=T_a)$ and $\Delta(f=T_a, T_s)$, ET_0-PM and $ET_0-\Delta$ in plain no-vegetation area (a, d, g), plain vegetation area (b, e, h) and mountainous area (c, f, i) of arid areas of Northwest China during 2003–2017. The purple shadow in the diagram represents the standard error for T_s , $\Delta(f=T_a, T_s)$ and $ET_0-\Delta$; the green shadow represents the standard error for T_a , $\Delta(f=T_a)$ and ET_0-PM . DOY, day of year.

4.2 Uncertainty caused by albedo

The mean surface albedo for more than 60% of the meteorological stations in the study area was determined to be less than 0.23. The coverage of vegetation in the arid regions of Northwest China is therefore notably less than the vegetation conditions pre-set by the PM method. The ET_0-PM , estimated by the PM method, was underestimated at almost 55% of the meteorological stations when compared with the ET_0-AB estimated using actual surface albedo (Fig. 4a). Although evaporation was strong in July and August, more than half of the meteorological stations were underestimated (Fig. 4b); this phenomenon, however, was not obvious.

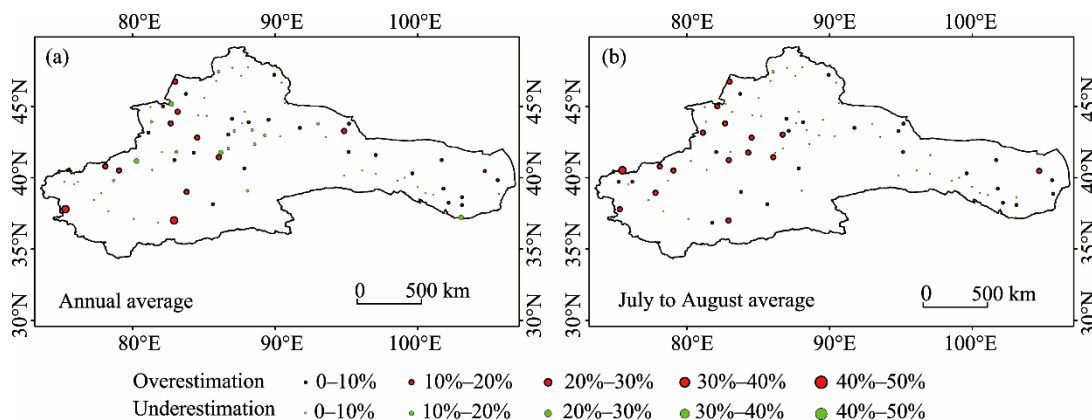


Fig. 4 Overestimation and underestimation of ET_0-PM and ET_0-AB (estimated by actual surface albedo) from 84 meteorological stations during 2003–2017

Next, we corrected the surface albedo of the study area (Fig. 5). The mountainous site had good vegetation coverage, and no obvious changes throughout the year. The actual surface albedo was closest to the fitted value of 0.23. Therefore, PM showed the smallest error in the estimation of ET_0 (Fig. 5a), with a mean difference of 3.3 mm/a. In the plain area, regardless of the degree of vegetation coverage, the surface albedo of the PM formula (0.23) resulted in a significant underestimation error of 44.6 mm/a (Figs. 5b and c). Interestingly, the estimation of evapotranspiration in the plain vegetation area was affected most by the surface albedo because of significant changes in vegetation coverage throughout the year. The mean underestimation was 45.2 mm/a, which accounted for 3.8% of the total potential evaporation (Figs. 5b and c). For the entire study area, changes in the surface albedo from July to August were not obvious. Therefore, the difference of ET_0 estimation, before and after surface albedo correction, was insignificant, and the overestimation difference for the whole area was 5.3 mm/a.

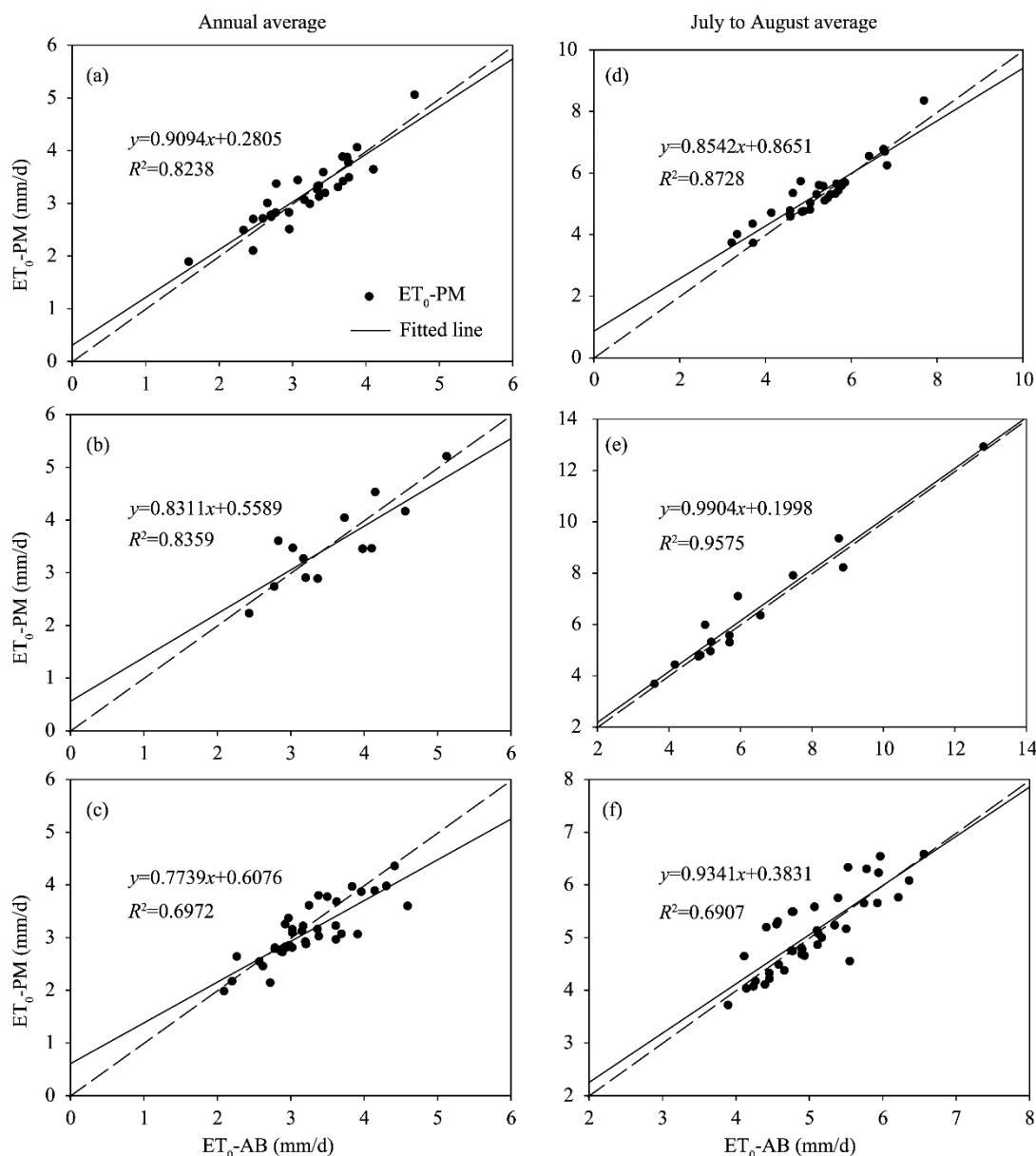


Fig. 5 Comparison of ET_0 -PM and ET_0 -AB in mountainous area (a, d), plain vegetation area (b, e) and plain no-vegetation area (c, f) of arid areas of Northwest China during 2003–2017

4.3 Uncertainty of the PM formula in arid areas

By simultaneously correcting the slope of the saturation vapor curve and the surface albedo, PM generally overestimated the potential evapotranspiration. Across the entire arid region, more than half of the sites overestimated potential evapotranspiration and more than 30% of the sites were overestimated by more than 100.0 mm/a (Fig. 6a). However, some sites were underestimated, although the number and degree of these differences were lower than the sites that were overestimated. The most extreme underestimated value was 323.3 mm/a, which was far smaller than the most extreme overestimated value of 681.5 mm/a. The same was true for the mean; differences between the underestimated and overestimated sites were 101.6 and 156.0 mm/a, respectively. In terms of the entire region, the mean annual overestimation was 33.7 mm/a; this phenomenon was more pronounced in July and August, with a mean overestimation of 29.2 mm/a.

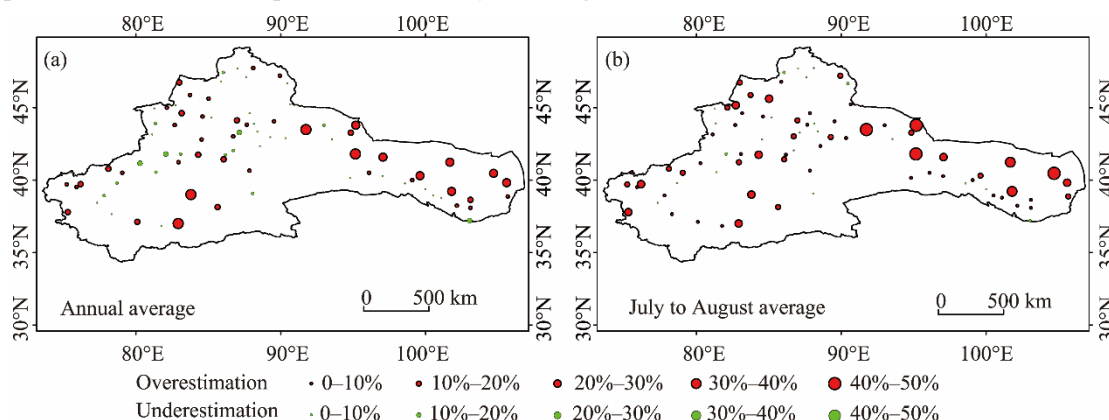


Fig. 6 Overestimation and underestimation of ET_0 -PM and ET_0 -Z (simultaneous correction of two parameters, the saturation vapor pressure and albedo) from 84 meteorological stations during 2003–2017

The overestimation of evapotranspiration by the PM formula showed significant spatial variability. The overestimation of the PM formula in the mountainous areas and plain non-vegetation areas was significant, but the difference in the plain vegetation area was not obvious. Among the difference, the average overestimation in the mountainous area was 57.9 mm/a, and the overestimation was 5%. The site with the highest overestimation of ET_0 was 456.1 mm/a. In the plain non-vegetation area, the mean overestimation was 124.0 mm/a, with an amplitude of 10%. The site with the highest overestimation had an ET_0 of 681.5 mm/a. The PM formula worked well in the plain vegetation area, with an annual underestimation of only 1.7% (Figs. 7a–c). Compared with the annual overestimation, the degree of overestimation for the PM formula was more significant in July and August. The overestimation of ET_0 in mountainous, plain non-vegetation and plain vegetation areas was 10%, 20% and 5%, respectively.

5 Discussion

5.1 Uncertainty of the PM method

Although the FAO-recommended PM method is widely used as a model to estimate evapotranspiration, many recent studies have highlighted that this method is associated with a large error in some areas (Dhungel et al., 2014). Chen et al. (2018) evaluated the uncertainty of PM method to estimate evapotranspiration in the temperate meadow region of Inner Mongolia using the eddy covariance method. Using reference parameters, the PM method overestimated ET by 12.1% and 12.8%, respectively, for half-hourly and daily values. In addition, the estimation error of the PM model in arid regions was also confirmed in the Heihe River Basin; monitoring of a corn field in this region showed that the PM method overestimated the latent heat flux during the dry season for the entire basin (Zhao et al., 2010). A significant body of research has attempted to address the source of error during the application of the PM method. A previous study estimated

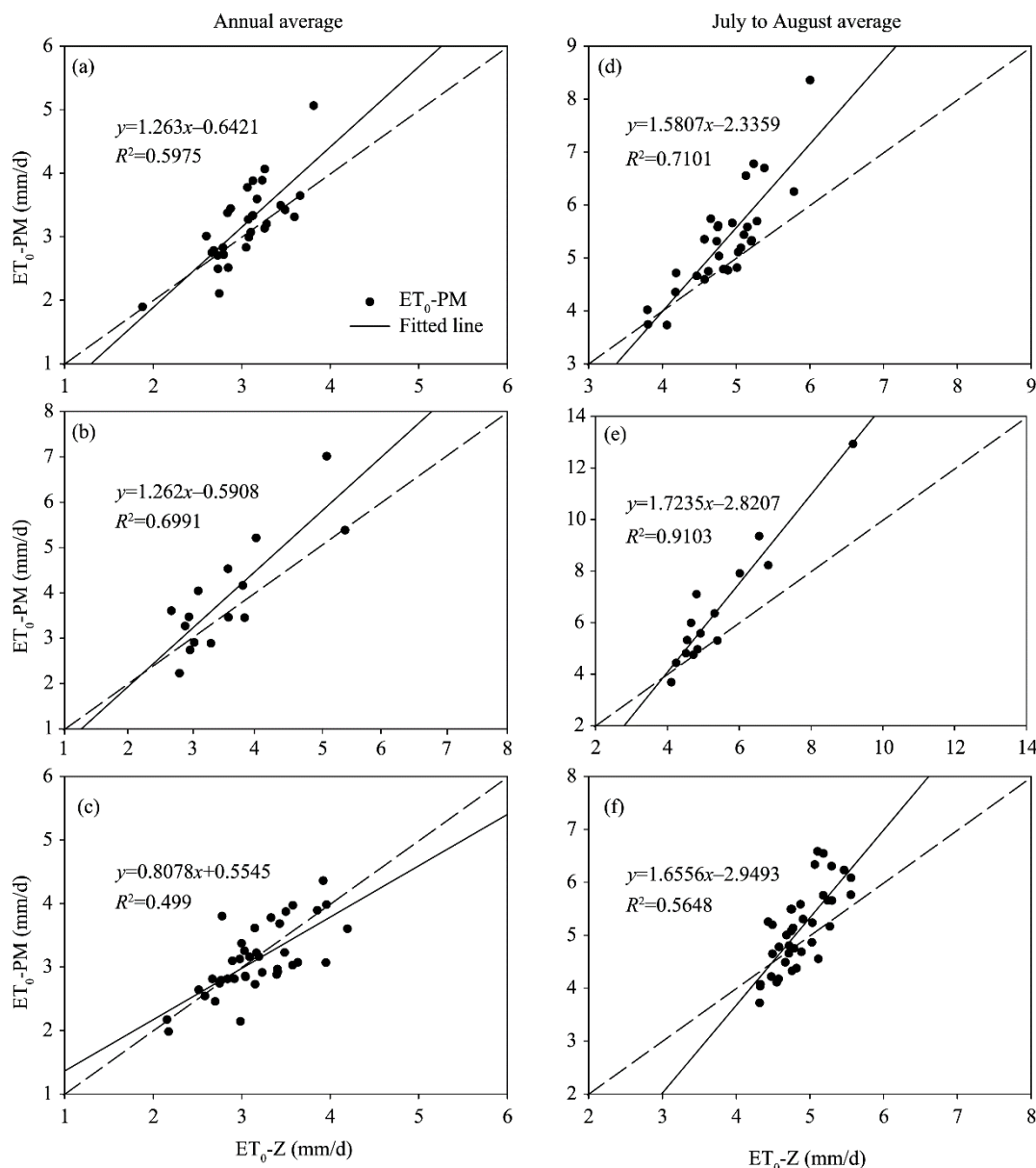


Fig. 7 Comparison of ET₀-PM and ET₀-Z in mountainous area (a, d), plain vegetation area (b, e) and plain no-vegetation area (c, f) of arid areas of Northwest China during 2003–2017

the error associated with rice field evapotranspiration in the PM model, and found that the general magnitude relationship, net radiation, soil heat flux, heat storage term, surface layer resistance and aerodynamic drag error rates, were 5%, 10%, 100%, 20% and 20%, respectively, and that the contribution rates of these to the overall calculation error for evapotranspiration were 26.8%, 5.36%, 53.6%, 11.11% and 3.17%, respectively (Liu et al., 2015). Sensitivity analysis of the reference evapotranspiration estimated by the PM method to meteorological factors, showed that ET₀ was most sensitive to the highest temperature, followed by relative humidity (Ali et al., 2009). In the present study, we corrected the slope of the saturation vapor curve, and the surface albedo. We found that the PM formula caused significant overestimation errors when applied for arid zones, and that this error was associated with clear temporal and spatial differences. Therefore, in arid regions, in which radiation and evaporation are strong, the correction of the radiation term, and the slope of the saturation vapor curve, cannot be ignored.

In addition, subsequent uncertainty analysis of the PM method for the estimation of combined satellite and ground-based evapotranspiration, carried out by Westerhoff (2015), showed that ET_0 was most sensitive to temperature and radiation terms, and that this sensitivity was related to its own ET_0 value. In the present study, we found that compared with the parameter-corrected method PM-Z, the error (ET_0-C), caused by the original PM method, showed strong correlations with the ET_0 values in arid regions (Fig. 8). In particular, the correlation coefficients for these two parameters were as high as 0.85 in July and August (Fig. 8b). Therefore, in areas with greater potential evapotranspiration, the PM method produced greater errors when applied for arid and semi-arid regions.

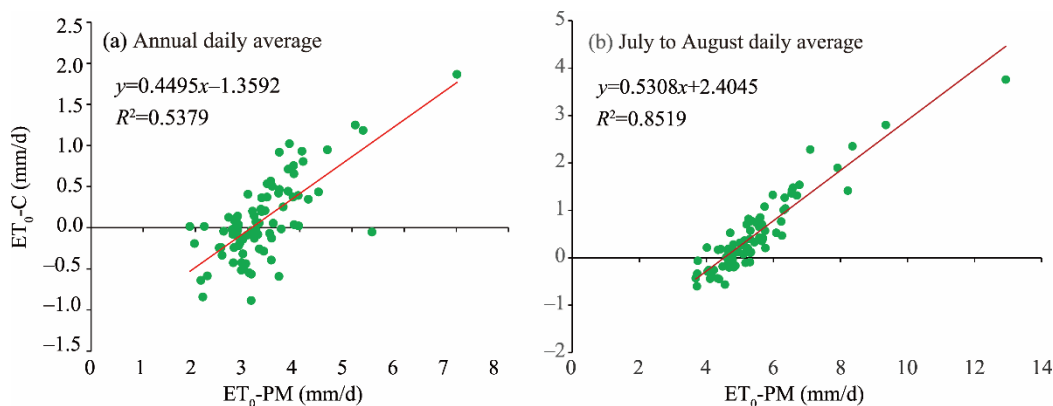


Fig. 8 Relationships of ET_0-PM with ET_0-C (the error caused by the original PM method) during 2003–2017

5.2 Potential impact of errors caused by PM method in arid areas

As an important aspect of the water cycle, evapotranspiration holds great significance for the calculation of land surface evaporation, water balance and crop water demand. Although the uncertainty relating to hydrological model input, and other parameters, provides a certain degree of tolerance to the model, the advantages of the PM method are fully evident (Oudin et al., 2006). A previous study, evaluating the effects of different potential evapotranspiration inputs on hydrological simulation results in northern Belgium, found that the use of the PM method led to an overestimation of runoff when using hydrological models (Samain and Pauwels, 2013). In addition, PM model-based evapotranspiration and MODIS evapotranspiration data were used as parameter inputs to compare hydrological simulations for the Mississippi River. These studies found that Nash-Sutcliffe efficiency was significantly higher when using MODIS evapotranspiration data (Parajuli et al., 2018). Further research is now required to investigate the specific reasons for this improvement.

In addition to the impact on runoff simulation, as an important aspect of plant water balance, evapotranspiration is critical to the accurate calculation of crop water requirements. Using experiments in France and New Zealand, the analysis of total sensitivity revealed that ET_0 explained the most variability in both irrigated maize water use, and rain-fed grain yield levels; soil evaporation was demonstrated to be of equal importance in the French experiment (Heidi et al., 2016). A slight error in crop water demand can result in a significant difference in water resource planning, such as agricultural irrigation water. This study selected two irrigation areas in the arid area and re-estimated the potential evaporation and crop water requirements over the past 13 a, as based on the revised PM formula. The uncertainty of the potential evapotranspiration estimated by the PM model led to overestimation of the crop water requirements during the growing season (Fig. 9). This directly caused the agricultural water demand in the two irrigation areas to be overestimated by 1.01×10^8 and 0.23×10^8 m³/a.

5.3 Parameter correction of the PM formula in a cross-environment

The PM model is an effective approach that is commonly used in evapotranspiration research

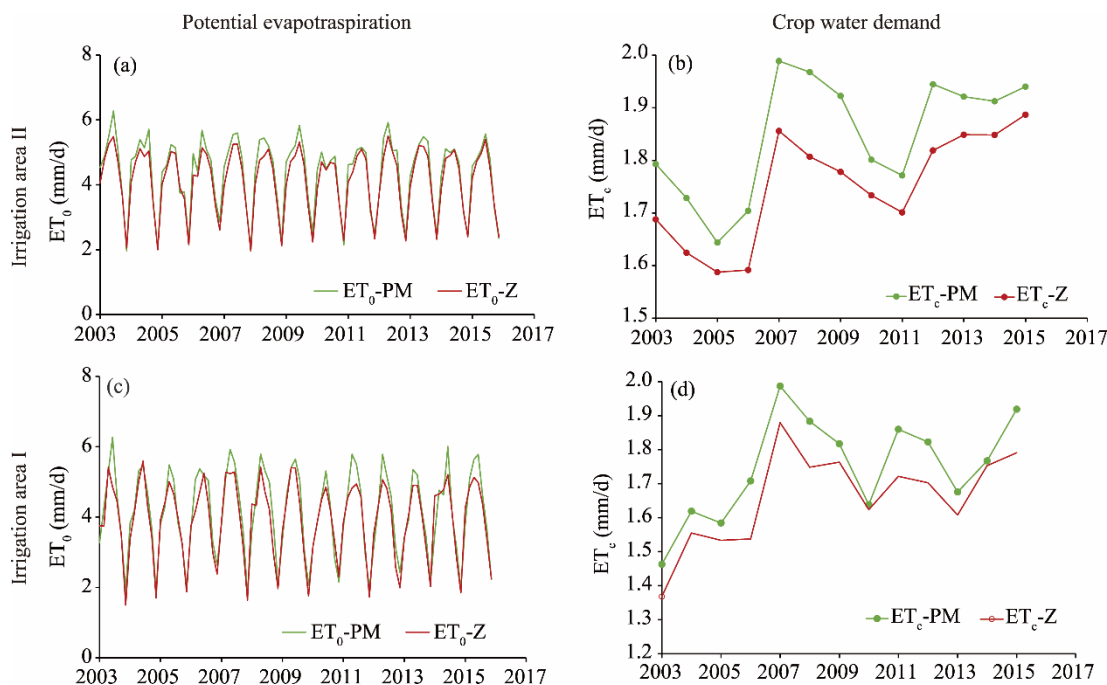


Fig. 9 Comparison of ET_0 -PM and ET_0 -Z for potential evapotranspiration trends, and ET_c -PM (based on PM model) and ET_c -Z (based on parameter correction) for crop water demand trends for the growth seasons of the two typical irrigation regions in the study area for the period 2003–2017

(Li et al., 2005). When using this calculation, scholars attempt to correct some of the parameters utilized by the model. However, due to the complexity and subjectivity of the observation procedure in obtaining the actual accurate value of the parameters, it is not easy to determine the extent of this error accurately and the parameters involved are difficult to determine. We have yet to arrive at a consensus of opinion with regards to how to determine these parameters. The Penman-Monteith (PM) model has performed well in verification calculation process in many parts of the world. For example, in California, the calculated ET_0 , and solar radiation hourly and daily data, were compared by linear regression for the PM and Hargreaves models; this analysis showed very high levels of correlation (Temesgen et al., 2005). Furthermore, the level of evapotranspiration simulated by the PM formula for the Heihe River Basin was in good agreement with the measured level of evapotranspiration. The coefficient of determination (R^2) for daily evapotranspiration simulation exceeds 0.8 (Wang and Ma, 2014); however, it is commonly known to the hydrological community that the PM method can produce errors when applied to sparsely vegetated areas. In order to improve the accuracy of the PM model, scientists are now re-fitting and adjusting certain parameters in accordance with the specific conditions associated with the study area. In arid areas, the accuracy of the PM method during the non-growth season was significantly improved when a soil moisture index algorithm was used instead of relative humidity (Sun et al., 2013); however this is difficult to apply under cross-environment conditions. As science and technology develops, some parameters (e.g., LST and Albedo) could be obtained by remote sensing, thus completely avoiding the error associated with parameter fitting; furthermore, this data could be applied to a complex cross-environment.

6 Conclusions

Vegetation coverage in the arid regions of Northwest China is very different from the vegetation conditions preset by the FAO. Furthermore, there is a large difference between the surface temperature and the air temperature. Therefore, this study used remote sensing data to obtain surface temperature data and restore the parameterized Δ formula. We also used remote sensing

albedo data to replace the fixed value of 0.23. We found that the Penman-Monteith (PM) model overestimated potential evapotranspiration in an arid zone (Fig. 10), and that the overestimation error was associated with significant differences in terms of temporal and spatial distribution. During our study period, compared with the ET_0 -Z, which was simultaneously corrected by temperature and surface albedo, the overestimation for ET_0 -PM was 33.7 mm/a; 86.5% of the difference occurred between July and August. With regard to spatial dynamics, this estimation error showed clear regional differences. The PM model showed an annual overestimation for potential evapotranspiration of 58 mm in the mountainous region, an underestimation of approximately 20.0 mm/a in the plain vegetation area, and an overestimation of 124.0 mm/a in the plain non-vegetation area.

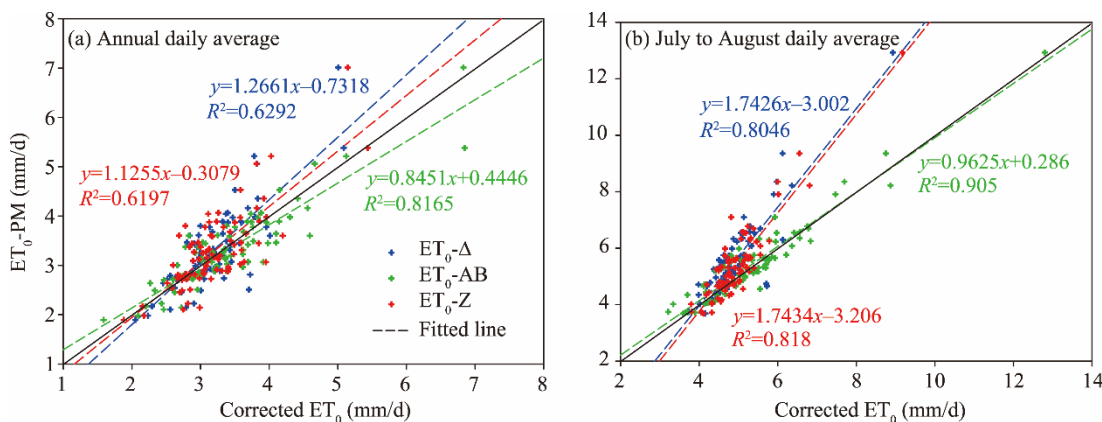


Fig. 10 Relationships of ET_0 -PM with corrected ET_0 , including ET_0 - Δ , ET_0 -AB and ET_0 -Z, during 2003–2017

Acknowledgements

This study was financially supported by the National Natural Science Foundation of China (41571109, 41601600). Appreciation goes to Mr. TAO Jintao for providing python code for preprocessing work on the meteorological data.

Reference

- Ali M H, Adham A K M, Rahman M M, et al. 2009. Sensitivity of Penman-Monteith estimates of reference evapotranspiration to errors in input climatic data. *Journal of Agrometeorology*, 11(1): 1–8.
- Allen R G, Pereira L G, Raes S M. 1998. Crop evapotranspiration guidelines for computing crop water requirements. FAO Irrigation and Drainage Paper No.56. FAO. Rome, Italy.
- Allen R G, Pruitt W O, Wright J L, et al. 2006. A recommendation on standardized surface resistance for hourly calculation of reference ET_0 by the FAO56 Penman-Monteith method. *Agricultural Water Management*, 81(1–2): 1–22.
- Anabalón A, Sharma A. 2017. On the divergence of potential and actual evapotranspiration trends: An assessment across alternate global datasets. *Earth Future*, 5(9): 905–917.
- Chen J E, Zuo H C, Wang Y, et al. 2014. Parameterization scheme about albedo changing with solar altitude angle over different underlying surface in arid areas of Northwest China. *Plateau Meteorology*, 33(1): 80–88. (in Chinese)
- Chen N N, Zhang Y S, Jin C J, et al. 2018. Intercomparison of three methods to estimate evapotranspiration over temperate meadow in Inner Mongolia: Penman–Monteith, Makkink and Priestley–Taylor equation. *Water and Environment*, 32(4): 500–507.
- Chen Y, Li Z, Fan Y T, et al. 2015. Progress and prospects of climate change impacts on hydrology in the arid region of Northwest China. *Environmental Research*, 139: 11–19.
- Chen Y, Li B F, Li Z, et al. 2016. Water resource formation and conversion and water security in arid region of Northwest China. *Journal of Geographical Sciences*, 26(7): 939–952.
- Ci J H, Feng Q, Zhang X Y, et al. 2005. Research progress on surveying and calculation of evapotranspiration of plants and its prospects. *Advances in Water Science*, 16(3): 450–459.
- Dhungel R, Allen R G, Trezza R, et al. 2014. Comparison of latent heat flux using aerodynamic methods and using the penman-

- monteith method with satellite-based surface energy balance. *Remote Sensing*, 6(9): 8844–8877.
- Ficklin D L, Letsinger S L, Ghoilzadeh H, et al. 2014. Incorporation of the Penman-Monteith potential evapotranspiration method into a Palmer Drought Severity Index Tool. *Computers & Geosciences*, 85: 136–141.
- Fugazza D, Senese A, Azzoni R S, et al. 2016. Spatial distribution of surface albedo at the Forni Glacier (Stelvio National Park, Central Italian Alps). *Cold Regions Science and Technology*, 125: 128–137.
- Hao X M, Zhang S H, Li W H, et al. 2018. The uncertainty of Penman-Monteith method and the energy balance closure problem. *Journal of Geophysical Research-Atmospheres*, 123(14): 7433–7443.
- Heidi W, Thomas G, Roelof O, et al. 2016. Uncertainty in future irrigation water demand and risk of crop failure for maize in Europe. *Environmental Research Letters*, 11(7): 074007, doi:10.1088/1748-9326/11/7/074007.
- Koffi D, Michael O, Curtis O, et al. 2018. Crop evapotranspiration, irrigation water requirement and water productivity of maize from meteorological data under semiarid climate. *Water*, 10(4): 405, doi: 10.3390/w10040405.
- Li L, Chi D C, Zhang Z L, et al. 2007. Analysis of the change characteristics and effect factors of reference evapotranspiration in Taizi River Basin. *Transactions of the Chinese Society of Agricultural Engineering*, 23(9): 34–38. (in Chinese)
- Li W L, Lu S H, Fu S M, et al. 2011. Numerical simulation of fluxes generated by inhomogeneities of the underlying surface over the Jinta Oasis in Northwestern China. *Advances in Atmospheric Sciences*, 28(4): 887–906.
- Li X G, Bi H X, Liu S, et al. 2005. Penman-Monteith evapotranspiration model and calculations of its parameters in forest underlying surface. *Research of Soil and Water Conservation*, 12(5): 257–261. (in Chinese)
- Li Z, Chen Y, Shen Y, et al. 2013. Analysis of changing pan evaporation in the arid region of Northwest China. *Water Resources Research*, 49(4): 2205–2212.
- Liu B, Hu J C, Zhao X L, et al. 2015. Error analysis on evapotranspiration estimation of paddy rice field by Penman-Monteith model. *Chinese Journal of Agrometeorology*, 36(1): 24–32. (in Chinese)
- Mallick K, Andrew J, Eva B, et al. 2014. A Surface Temperature Initiated Closure (STIC) for surface energy balance fluxes. *Remote Sensing of Environment*, 141: 243–261.
- Otles Z, Gutowski W. 2005. Atmospheric stability effects on Penman-Monteith evapotranspiration estimates. *Pure and Applied Geophysics*, 162(11): 2239–2254.
- Oudin L, Perrin C, Mathevet T, et al. 2006. Impact of biased and randomly corrupted inputs on the efficiency and the parameters of watershed models. *Journal of Hydrology*, 320(1–2): 62–83.
- Parajuli P B, Jayakody P, Ouyang Y. 2018. Evaluation of using remote sensing evapotranspiration data in swat. *Water Resources Management*, 32(3): 985–996.
- Peng H, Jia Y W, Qiu Y Q, et al. 2013. Assessing climate change impacts on the ecohydrology of the Jinghe River basin in the Loess Plateau, China. *Hydrological Sciences Journal*, 68(3): 651–670.
- Penman H L. 1948. Nature evaporation from open water, bare soil and grass. *Proceedings of the Royal A*, 193(1032): 120–145.
- Raoufi R, Beighley E. 2017. Estimating daily global evapotranspiration using Penman-Monteith equation and remotely sensed land surface temperature. *Remote Sensing*, 9(11): 1138, doi: 10.3390/rs9111138.
- Samain B, Pauwels V R N. 2013. Impact of potential and (scintillometer-based) actual evapotranspiration estimates on the performance of a lumped rainfall-runoff model. *Hydrology and Earth System Sciences*, 17(11): 4525–4540.
- Shen S H, Leptoukh G G. 2011. Estimation of surface air temperature over central and eastern Eurasia from Modis land surface temperature. *Environmental Research Letters*, 6(4): 045206, doi:10.1088/1748-9326/6/4/045206.
- Shen Y J, Chen Y N, Qi Y Q, et al. 2013. Estimation of regional irrigation water requirement and water supply risk in the arid region of Northwestern China 1989–2010. *Agricultural Water Management*, 128(1): 55–64.
- Sun L, Liang S L, Yuan W P, et al. 2013. Improving a Penman-Monteith evapotranspiration model by incorporating soil moisture control on soil evaporation in semiarid areas. *International Journal of Digital Earth*, 6(S1): 134–156.
- Tegos A, Malamos N, Efstratiadis A. et al. 2017. Parametric modelling of potential evapotranspiration: a global survey. *Water*, 9(10): 795, <https://doi.org/10.3390/w9100795>.
- Temesgen B, Eching S, Davidoff B. 2005. Comparison of some reference evapotranspiration equations for California. *Journal of Irrigation and Drainage Engineering*, 131(1): 73–84.
- Tirivarombo S, Osupile D, Eliasson P. 2018. Drought monitoring and analysis: Standardised Precipitation Evapotranspiration Index (SPEI) and Standardised Precipitation Index (SPI). *Physics and Chemistry of the Earth, Parts A/B/C*, 106: 1–10.
- Wan Z, Li Z L. 2008. Radiance-based validation of the V5 MODIS land-surface temperature product. *International Journal of Remote Sensing*, 29(17–18): 5373–5395.
- Wang H B, Ma M G. 2014. Estimation of transpiration and evaporation of different ecosystems in an inland river basin using remote sensing data and the Penman-Monteith equation. *Acta Ecologica Sinica*, 34(19): 5617–5626. (in Chinese)
- Wei X, Wei Z W, Wen X F. 2018. Evapotranspiration partitioning at the ecosystem scale using the stable isotope method-A review.

- Agricultural and Forest Meteorology, 263: 346–361.
- Westerhoff R S. 2015. Using uncertainty of Penman and Penman–Monteith methods in combined satellite and ground-based evapotranspiration estimates. *Remote Sensing of Environment*, 169: 102–112.
- Xu C Y, Singh V P. 2001. Evaluation and generalization of temperature-based methods for calculating evaporation. *Hydrological Processes*, 15(2): 305–319.
- Zhang F H. 2003. Oasis agriculture characters and development in arid area of Northwestern China. *Journal of Arid Land Resources & Environment*, 17(4): 19–23. (in Chinese)
- Zhang J, Sun F, Xu J. 2015. Dependence of trends in and sensitivity of drought over China (1961–2013) on potential evaporation model. *Geophysical Research Letters*, 43(1): 206–213.
- Zhang R H, Du J P, Sun R. 2012. Review of estimation and validation of regional evapotranspiration based on remote sensing. *Advance in Earth Sciences*, 27(12): 1295–1307. (in Chinese)
- Zhao L L, Xia J, Xu C Y, et al. 2013. A review of evapotranspiration estimation methods in hydrological Models. *Journal of Geographical Sciences*, 68(1): 127–136.
- Zhao W Z, Ji X B, Kang E S, et al. 2010. Evaluation of Penman-Monteith model applied to a maize field in the arid area of Northwest China. *Hydrology and Earth System Sciences*, 14(7): 1353–1364.